THE JOURNAL OF PHYSICAL CHEMISTRY B

Article

pubs.acs.org/JPCB

Sign Crossover in All Maxwell–Stefan Diffusivities for Molten Salt LiF-BeF_2: A Molecular Dynamics Study

Brahmananda Chakraborty*

High Pressure and Synchrotron Radiation Physics Division, Bhabha Atomic Research Centre, Trombay, Mumbai 400085, India

Supporting Information

ABSTRACT: Applying Green–Kubo formalism and equilibrium molecular dynamics (MD) simulations, we have studied for the first time the dynamic correlation, Onsager coefficients, and Maxwell–Stefan (MS) diffusivities of molten salt LiF-BeF_2, which is a potential candidate for a coolant in a high temperature reactor. We observe an unusual composition dependence and strikingly a crossover in sign for all the MS diffusivities at a composition of around 7% of LiF where the MS diffusivity between cation–anion pair ($Đ_{BeF}$ and $Đ_{LiF}$) jumps from positive to negative value while the MS diffusivity between cation–cation pair ($Đ_{LiBe}$) becomes positive from a negative value. Even though the negative MS diffusivities have been observed for electrolyte solutions between cation–cation pair, here we report negative MS diffusivity between cation–anion pair where $Đ_{BeF}$ shows a sharp rise around 66% of BeF_2, reaches maximum value at 70% of BeF_2, and then decreases almost exponentially with a sign change for BeF_2 around 93%. For low mole fraction of LiF, $Đ_{BeF}$ follows the Debye–Huckel theory and rises with the square root of LiF mole fraction similar to the MS diffusivity between cation–anion pair in aqueous solution of electrolyte salt. Negative MS diffusivities while unusual are, however, shown to satisfy the non-negative entropy constraints at all thermodynamic states as required by the second law of thermodynamics. We have established a strong correlation between the structure and dynamics and predict that the formation of flouride polyanion network between Be and F ions and coulomb interaction is responsible for sharp variation of the MS diffusivities which controls the multicomponent diffusion phenomenon in LiF-BeF_2 which has a strong impact on the performance of the reactor.

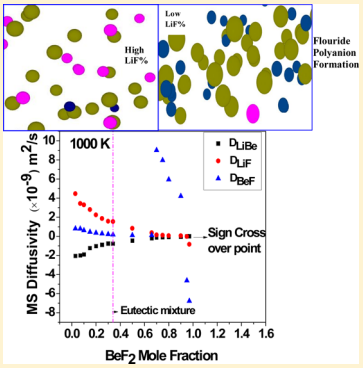

1. INTRODUCTION

Molten salt LiF-BeF_2 is a potential candidate for coolant in high temperature reactors[1] and is considered in the design of an advanced high temperature reactor (AHTR).[2] Fluoride salts are preferred over chloride salt due to their lower neutron absorption cross-section, higher irradiation stability, higher volumetric heat capacity, and very low vapor pressures with boiling points in excess of 1400 °C and can dissolve high concentrations of actinides and fission products.[3,4] The structure and dynamics of the molten salt at operating temperature and pressure have a strong impact on the performance of the reactor. Matsumiya et al.[5] carried out MD simulations to study electric properties of various chloride and fluoride salts. They computed the self-exchange velocity and self-diffusion coefficient in molten alkali quaternary chlorides and fluorides. Agarwal et al.[6] studied the thermodynamic properties of liquid beryllium difluoride BeF_2 through molecular dynamics (MD)[7] simulations using transferable rigid ion model potential. They predicted an anomalous increase of excess entropy with isothermal compression at low temperatures leading to diffusional as well as structural anomalies resembling those in water. Kanian et al.[8] studied the dynamics of molten LiF-KF mixtures using MD simulations and nuclear magnetic resonance (NMR) measurements. They computed the self-diffusion coefficients of fluorine, lithium, and potassium across the full composition range at 1123 K and predicted that the composition affects the self-diffusion of anions and cations more weakly than the temperature. Jabes[9] et al. reported the structure and transport properties of LiF-BeF_2 through MD simulations using rigid and polarizable ion potential. All of the above studies were restricted to self-diffusion only, the multicomponent diffusional properties, which are critical to the nuclear and chemical applications, have not been addressed in great detail so far. Recently Chakraborty et al.[10] studied the multicomponent diffusion in molten LiCl-KCl and reported negative and divergent Maxwell–Stefan (MS) diffusivity for positive–positive ion pairs. But so far there is no data for multicomponent diffusional properties of molten salt LiF-BeF_2 although it has tremendous application in the nuclear industry.

Although diffusion[11,12] in binary systems has been studied extensively not much attention has been given for the diffusion in ternary and higher order systems. This is because the theory of diffusion for multicomponent systems is very complicated and its complexity goes far beyond the apparent simplicity of Fick's law. In an n component system the generalized Fick's law[13−15] with respect to a molar reference frame is given by

Received: May 18, 2015
Revised: July 7, 2015
Published: July 20, 2015

DOI: 10.1021/acs.jpcb.5b04713
J. Phys. Chem. B 2015, 119, 10652−10663

$$J_i = -C_t \sum_{j=1}^{n-1} D_{ij} \nabla x_j \quad (1)$$

in which J_i is the diffusion flux, C_t is the total molar concentration, D_{ij} are Fick diffusivities, and ∇x_j is the gradient in mole fraction of component j. So in an n component system there are $(n-1)^2$ Fick diffusion coefficients with non-symmetric matrix elements which often depend strongly on the composition. The form of this matrix has been a subject of limited theoretical studies.[16−21] Another important factor to decide the suitable approach for multicomponent diffusion is the system we are going to study. In molten salt LiF-BeF_2, the ions Li^+ and F^- and Be^{2+} diffuse simulataneously driven by activity, electrical, and maybe pressure gradients. Although the form of Fick's law[13] appears to be simple and it is the starting point for mass transfer, it cannot be applied in electrolyte solutions because it neglects the effect of electric fields.[22] In a mixture of HCl and NaCl, due to the electric field generated by H^+ ions, sodium chloride diffuses against its gradient, in the direction opposite to what we expect from Fick's law.[23] This phenomenon can be correctly modeled only with the MS[14] approach. Another approach by Nernst−Planck,[24] although it takes the electrical effects into account and is the preferred starting point for mass transfer in electrochemistry, neglects activity and pressure gradients. Nernst−Planck[24] approach can be considered as in between Fick's and MS approach. In the MS approach the driving force takes account of activity, electrical and pressure gradient and provides a physically based comprehensive framework for describing multicomponent mass transport where diffusion coefficients are symmetric and $n(n-1)/2$ MS diffusivities are sufficient to describe diffusion in an n-component system. In the MS framework, the driving force for diffusion of component i is balanced by the frictional force bewteen the component i and other components resulting in the following equation:[14]

$$-\frac{1}{RT}\nabla\mu_i = \sum_{\substack{j=1 \\ j\neq i}}^{n} \frac{x_j(u_i - u_j)}{Đ_{ij}} \quad (2)$$

where MS diffusivity $Đ_{ij}$ has the physical significance of an inverse drag force. The MS framework is preferred over that of Fickian diffusion in theoretical, computational, and experimental analyses due to the fewer number of diffusion coefficients, empirical correlation to self−diffusivities that aid in model development, relatively smaller dependence on concentrations, and in most cases, a symmetric, quasi-positive, diffusivity matrix.[25] However, as the experiment cannot measure the chemical potential directly, it is difficult to get MS diffusivity from the experiments. It is general practice to transform MS diffusivities to Fickian diffusivities using the thermodynamic factors that arise from the nonideality of the multicomponent system.[14,26,27]

In this manuscript, we report for the first time MS diffusivities for molten salt LiF-BeF_2 mixture at eutectic composition in the temperature range 750−1500 K and at 1000 K in the composition range 3−95% LiF using Green−Kubo formalism[28] and equilibrium molecular dynamics (MD) simulations. We observe a crossover in sign for all the MS diffusivities in ternary mixture LiF-BeF_2 at composition around 7% LiF, where the MS diffusivity between cation−anion pair ($Đ_{BeF}$ and $Đ_{LiF}$) jumps from positive to negative value while the MS diffusivity between cation−cation pair ($Đ_{LiBe}$) becomes positive from negative value. Negative MS diffusivity, although unusual, has been reported in few cases for electrolyte solutions[10] and in ion exchange membrane[29] for positive-positive ion pairs. In addition to negative MS diffusivity between positive−positive ion pairs we observe that MS diffusivity between positive−negative ion pairs also becomes negative for small mole fraction of LiF. Although the MS diffusivities are expected to depend very lightly on the composition due to decoupling of thermodynamic factor, the diffusivity $Đ_{Be-F}$ decreases sharply for lower concentration of LiF. Negative MS diffusivity for both positive−positive and positive−negative ion pairs satisfy the non-negative entropy production[29] imposed by the second law of thermodynamics. Interestingly, the entropy production rate follows a Gausian pattern with the mole fraction of LiF in the mixture. We have observed a strong correlation between the structure and dynamics and related it to resolve the unusual composition dependence of LiF-BeF_2 mixture.

2. THEORETICAL APPROACH

In this section, we will present the approach adapted to compute the Onsager matrix containing the phenomenological coefficient for multicomponent diffusion from the Green−Kubo[28] formulas derived in the barycentric reference frame. The formalism is based on linear response theory where MD simulations are used to calculate Onsager coefficients[30] in an n component system. The diffusion is considered in an isothermal and isobaric system driven only by the chemical-potential gradient. According to the linear phenomenological theory, the diffusive fluxes in a multicomponent system with n species are linear homogeneous functions of thermodynamic forces as given by[31,32]

$$\hat{\mathbf{J}} \equiv \mathbf{\Lambda}\hat{\mathbf{X}} \quad (3)$$

where $\hat{\mathbf{J}}$ and $\hat{\mathbf{X}}$ are the diffusive flux and thermodynamic force vectors, respectively, and Λ is the Onsager matrix containing the phenomenological coefficients. The detailed theoretical formulizm is described in ref 10 and here we will outline the steps to compute MS diffusivity. The elements of the Onsager dynamical matrix can be obtained from diffusive mass flux correlation and expressed as[30]

$$\Lambda^0_{ik} = \frac{1}{3N}\int_0^\infty \mathrm{d}t\, \langle \mathcal{J}^0_i(t)\mathcal{J}^0_k(0)\rangle \equiv \frac{1}{3N}\int_0^\infty \mathrm{d}t\, \Psi^0_{ik}(t) \quad (4)$$

where N is the total number of atoms/ions in the system, $\Psi(t)$ represents the ensemble average of the diffusive mass flux correlation and the superscript 0 indicates that it is in barrycentric referrence frame. The volume averaged diffusive flux is basically the sum of the atom velocities relative to the barycentric velocity which is constrained to be zero and is expressed by[32]

$$\mathcal{J}^0_k(t) = \int_\Omega \mathbf{j}_k(\mathbf{r}, t) = \sum_{l=1}^{N_k} [\mathbf{u}^l_k(t) - \mathbf{V}^0(t)] \quad (5)$$

The Onsager matrix elements can be also determined from the atomic displacements using Einstein's form as given by[33]

$$\Lambda^0_{ik} = \frac{1}{6N}\lim_{t\to\infty}\frac{\mathrm{d}}{\mathrm{d}t}\langle[\mathbf{r}^0_i(t) - \mathbf{r}^0_i(0)]\cdot[\mathbf{r}^0_k(t) - \mathbf{r}^0_k(0)]\rangle \quad (6)$$

where $\mathrm{r}_i{}^0(t)$ is the position of the i^{th} particle at time t in barrycentric referrence frame.

DOI: 10.1021/acs.jpcb.5b04713
J. Phys. Chem. B 2015, 119, 10652−10663

The Einstein's form in eq 6 is equivalent to Green−Kubo form in eq 5. The expression for MS diffusivity in eq 2 can also be written in terms of molar fluxes relative to the mean molar velocity as[14]

$$-\frac{x_i}{RT}\nabla\mu_i = \sum_{\substack{k=1\\k\neq i}}^{n}\frac{1}{c\mathcal{D}_{ik}}(x_k\mathbf{J}_i^{\bullet} - x_i\mathbf{J}_k^{\bullet}) \tag{7}$$

and transformed into a matrix form as

$$\hat{\mathbf{X}}^{\bullet} = \mathbf{B}\hat{\mathbf{J}}^{\bullet} \tag{8}$$

where $\hat{\mathbf{X}}^{\bullet}$ and $\hat{\mathbf{J}}^{\bullet}$ are vectors of dimension $(n-1)$ and $\mathbf{B}$ is a $(n-1)$ by $(n-1)$ matrix, the elements of which are given by[34]

$$B_{ij} = \delta_{ij}\left(\frac{x_i}{\mathcal{D}_{in}} + \sum_{\substack{k=1\\k\neq i}}^{n}\frac{x_k}{\mathcal{D}_{ik}}\right) + (1-\delta_{ij})x_i\left(\frac{1}{\mathcal{D}_{in}} - \frac{1}{\mathcal{D}_{ij}}\right) \tag{9}$$

where δ_{ij} is the Kronecker delta function. Equation 8 can be now inverted to give

$$\hat{\mathbf{J}}^{\bullet} = \mathbf{B}^{-1}\hat{\mathbf{X}}^{\bullet} \equiv \hat{\mathbf{\Lambda}}^{\bullet}\hat{\mathbf{X}}^{\bullet} \tag{10}$$

By comparing eqs 3 and 10, we can see that the Onsager matrix is equivalent to $\mathbf{B}^{-1}$. In the above equation the Onsager matrix elements are in the mean molar velocity frame whereas in MD simulation we compute Onsager matrix in barycentric referrence frame with $n \times n$ Onsager coefficients. Following appropriate transformation of the reference frame and dimension reduction from n to $(n-1)$, $\mathbf{K}$ $(\equiv\mathbf{B}^{-1})$ matrix elements for a ternary system can be written in terms of Onsager coefficients as[34]

$$K_{11} = (1-x_1)\left(\frac{\Lambda_{11}}{x_1} - \frac{\Lambda_{13}}{x_3}\right) - x_1\left(\frac{\Lambda_{21}}{x_1} - \frac{\Lambda_{23}}{x_3} + \frac{\Lambda_{31}}{x_1} - \frac{\Lambda_{33}}{x_3}\right)$$

$$K_{12} = (1-x_1)\left(\frac{\Lambda_{12}}{x_2} - \frac{\Lambda_{13}}{x_3}\right) - x_1\left(\frac{\Lambda_{22}}{x_2} - \frac{\Lambda_{23}}{x_3} + \frac{\Lambda_{32}}{x_2} - \frac{\Lambda_{33}}{x_3}\right)$$

$$K_{21} = (1-x_2)\left(\frac{\Lambda_{21}}{x_1} - \frac{\Lambda_{23}}{x_3}\right) - x_2\left(\frac{\Lambda_{11}}{x_1} - \frac{\Lambda_{13}}{x_3} + \frac{\Lambda_{31}}{x_1} - \frac{\Lambda_{33}}{x_3}\right)$$

$$K_{22} = (1-x_2)\left(\frac{\Lambda_{22}}{x_2} - \frac{\Lambda_{23}}{x_3}\right) - x_2\left(\frac{\Lambda_{12}}{x_2} - \frac{\Lambda_{13}}{x_3} + \frac{\Lambda_{32}}{x_2} - \frac{\Lambda_{33}}{x_3}\right) \tag{11}$$

After obtaining the $\mathbf{B}$ matrix through $\mathbf{K}$ $(\equiv\mathbf{B}^{-1})$ matrix finally the MS diffusivities are obtained using eq 9 and for ternary mixture expressed as

$$\mathcal{D}_{12} = \left[B_{11} - \left(1 + \frac{x_3}{x_1}\right)B_{12}\right]^{-1}$$

$$\mathcal{D}_{23} = \left[B_{22} + \left(\frac{x_1}{x_2}\right)B_{21}\right]^{-1}$$

$$\mathcal{D}_{13} = \left[B_{11} + \left(\frac{x_2}{x_1}\right)B_{12}\right]^{-1} \tag{12}$$

3. COMPUTATIONAL METHOD

In order to compute the Onsager phenomenological coefficients for ternary systems we have developed various modules using mass flux and mean square displacement formulation and incorporated these modules to MD code DL_POLY_4.[35] From Onsager phenomenological coefficients MS diffusivities are obtained using an in-house code. The molecular configurations for various compositions were generated using PACKMOL[36] software which introduces ions in a cubic box. MD simulations are performed with 4000−6000 ions (for various compositions) in a cubic cell with periodic boundary conditions where the ions interact through a Born−Mayer−Huggins (BHM) short−ranged potential, originally developed by Fumi and Tosi.[37] The functional form of the potential is given by

$$\Phi_{ij}^{\text{short}} = B_{ij}e^{-\alpha r_{ij}} - \frac{C_{ij}}{r_{ij}^{6}} - \frac{D_{ij}}{r_{ij}^{8}} \tag{13}$$

where r_{ij} is the interionic separation between two ions, i and j, and α, B, C, and D are constants. The first term is the exponential repulsion term, the second and third terms account for the dipole−dipole interaction and dipole-quadruple interactions, respectively. The parameters used for the eutectic mixture are given in a table in Supporting Information. The BHM potential is successfully used in predicting several thermodynamic, structural, and transport properties of molten salts[38,39] and is comparable to polarizable models that are derived from ab initio simulations.[40] Jabes[9] et al. concluded that for liquid LiF−BeF_2 the structural correlations, ionic conductivity, viscosity and self-diffusivity computed using this potential matches nicely with first-principles-based, polarizable ion models. The limitation of the potential is that the densities obtained with this potential are approximately 17−20% lower than the experimental value. In addition to this we have long-range coulomb interactions. The short-range interaction is strongest between the F−F pair and weakest for the Li−Li pair as shown in the Figure 1. In general, the ion pairs containing F ions interact more strongly. To find the equilibrium density the system is first equilibrated in an NPT ensemble for 500 ps followed by another 100 ps for taking the average and the dynamical correlations were collected in an NVT ensemble for 300 ps. In order to improve the statistics we have used overlapped data structure[41] where the Onsager coefficients are computed by averaging over 3000 independent data set in each run and having six independent runs for each composition. The Newton's equations of motion are integrated by the Velocity Verlet algorithm using a time step of 1 fs and the electrostatic interactions are modeled by Ewald sum with a cut−off radius of 18 Å.

DOI: 10.1021/acs.jpcb.5b04713
J. Phys. Chem. B 2015, 119, 10652−10663

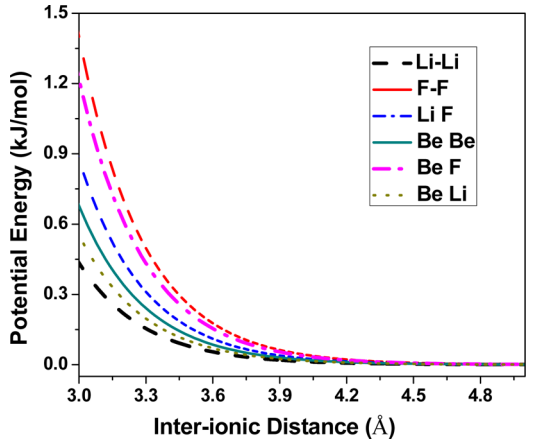

Figure 1. Short−ranged BHM interactions for LiF-BeF_2 mixture.

4. RESULTS AND DISCUSSION

4.1. Diffusive Flux Correlations and Onsager Coefficients. First we have optimized the density of the salt mixture at different temperatures and compositions using NPT ensemble. The optimized density for the mixture with 50% LiF at 1123 K is 1.523 g/cm^3, which is in excellent agreement with the computed value of 1.503 g/cm^3 by Jabes[9] et al. using similar transferable rigid-ion model (TRIM) potential which is the sum of Coulombic interactions and Born−Mayer−Huggins (BHM) short-ranged potential. The optimized density is however smaller than the experimental density of 1.873 g/cm^3 reported by Cantor et al.[42] In order to study the dynamics of the ions in Figure 2a we present the temporal variation of the diffusive flux correlations for eutectic mixture (66% LiF) at a temperature of 750 K. We observe prominent backscattering or cage effect, which is alternate negative and positive flux correlations after the initial decay for almost all correlations at 750 K. The caging effect is formed by the obstruction from the neighboring ions and it indicates trapping of the ions. The area constructed by the diffusive flux correlations with the X axis is proportional to the diffusivity of the species. The backscattering is strongest for Be−Be and Be−F ion pairs and weakest for Li−Li ions pair follwed by Li−F. So Li−Li ion pair diffuses much faster which is also corroborated by the fact that the Onsager coefficient L_{LiLi}, which is the integral of diffusive flux correlations, have the highest magnitude as shown in the Figure 2c. The correlation for Li−F ion pair starts with a negative value owing to which it has negative Onsager coefficient having magnitude just below that of Li−Li ion pair. Due to strong backscattering the ion pairs Be−Be and Be−F diffuse very slowly and have the least magnitude of the Onsager coefficient.

When the temperature is increased to 1123 K, although the cage effect diminishes for Li−Li, Li−Be, and Li−F ion pairs, we observe persistance of cage dynamics for Be−Be and Be−F ion pairs over the temperature as shown in Figure 2b. So the ions Be and F remains in entrapment even at higher thermal energy and there is no noticeable change in the Onsager coefficients L_{BeBe} and L_{BeF} over the temperature as shown in Figure 2c. Overall the Onsager coefficient increases with temperature for the pair involving Li and remains almost the same for Be−Be, Be−F, and F−F ion pairs.

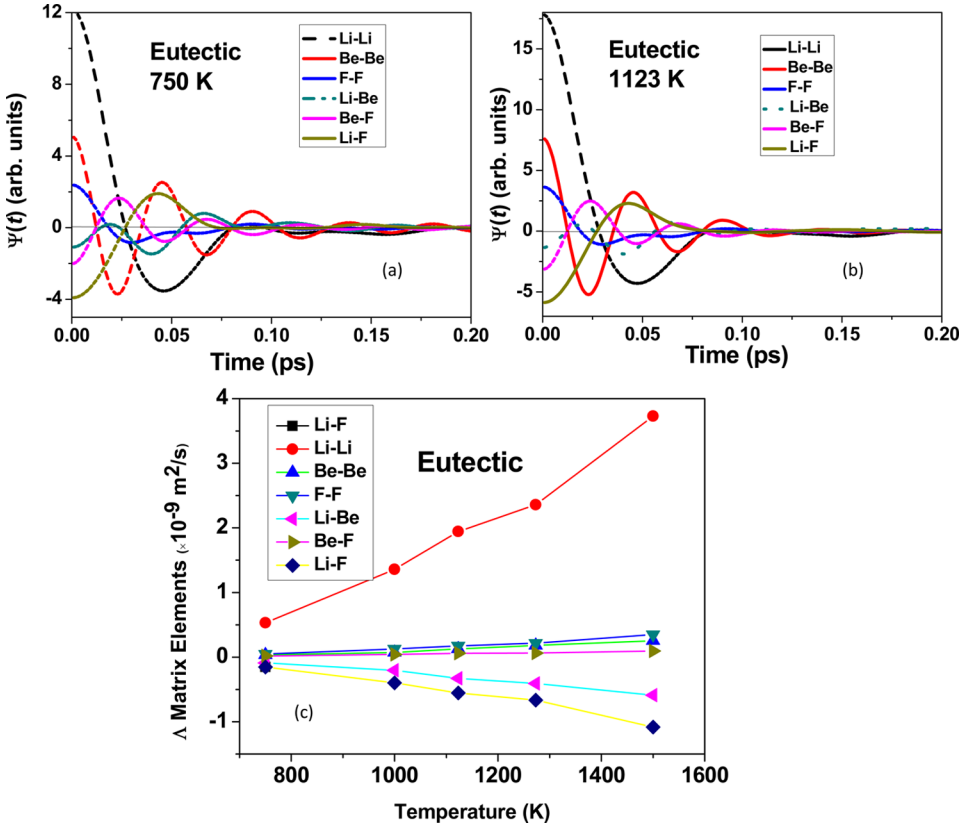

Figure 2. Temporal variation of diffusive flux correlation, $\Psi(t)$, at (a) 773 K and (b) 1123 K. (c) Variation of Onsager coefficients (Λ matrix elements) with temperature at eutectic composition.

DOI: 10.1021/acs.jpcb.5b04713
J. Phys. Chem. B 2015, 119, 10652−10663

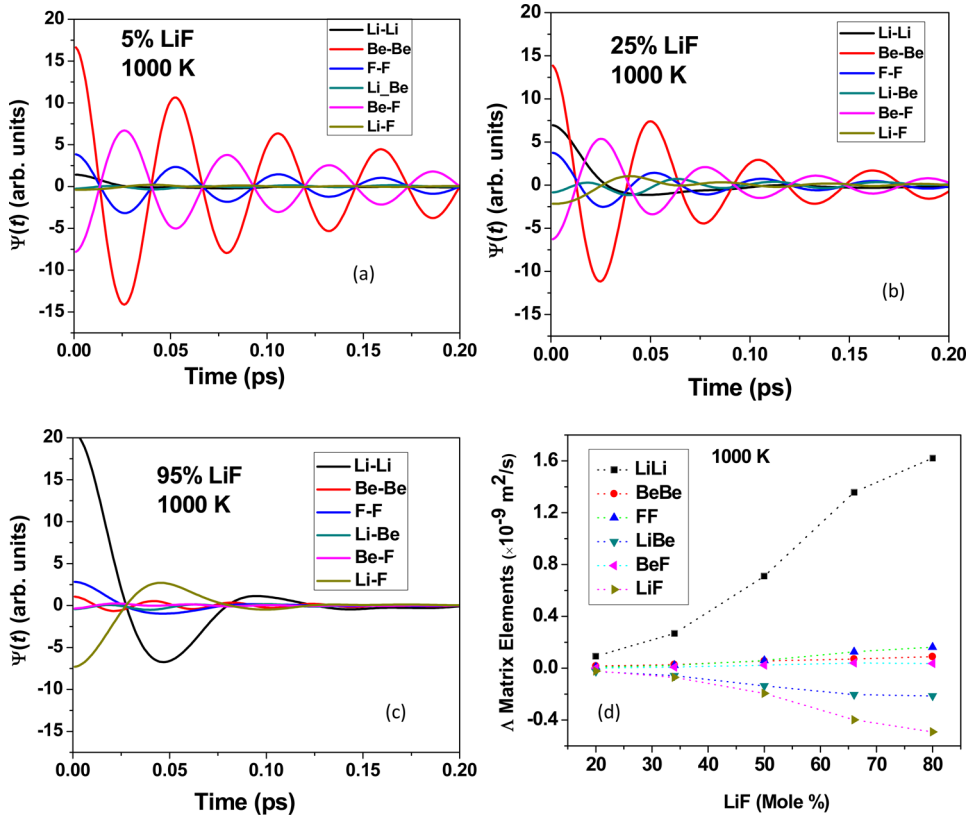

Figure 3. Temporal variation of diffusive flux correlation, $\Psi(t)$, at 1000 K for composition (a) 5% LiF, (b) 25% LiF, and (c) 95% LiF. (d) Variation of Onsager coefficients (Λ matrix elements) with composition at temperature 1000 K.

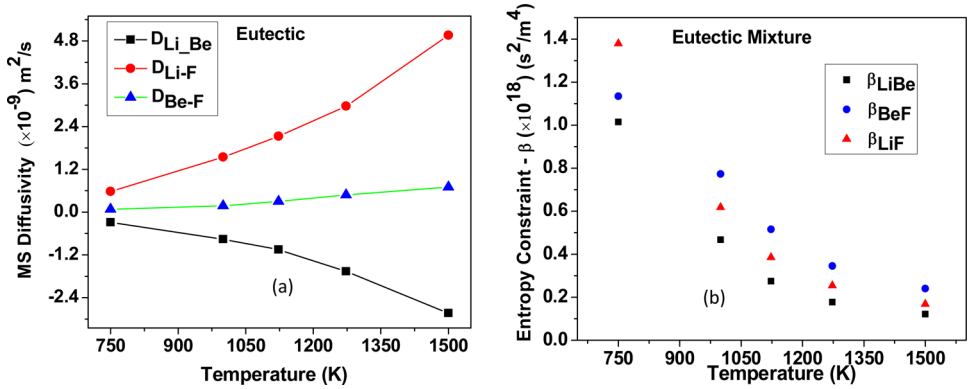

Figure 4. (a) Variation of MS diffusivities with temperatures at eutectic composition. (b) Variation of Entropy constraint with temperature showing a non−negative entropy production rate.

Now we will discuss the temporal variation of diffusive flux correlations for different composition at a temperature of 1000 K. Figure 3a−c potrays diffusive flux correlations for LiF mole fraction of 0.05, 0.25, and 0.95 at 1000 K. For the 5% LiF mixture, we observe strong backscattering for Be−Be, Be−F, and F−F ion pairs signifying poor diffusion of these species in the presence of strong entrapment. Although there is no cage dynamics for the ion pairs containing Li ion their movement is too slow as indicated by the small area covered by diffusive flux correlations with the X axis. So in BeF_2 rich salt the diffusivity of all the species is very low making the salt sluggish. As the LiF concentration increases to 25%, the cage dynamics for Be−Be, Be−F, and F−F ion pairs remains significantly strong whereas Li ions become more dynamic. As a result there is no noticeable change for the Onsager coefficients L_{BeBe}, L_{FF}, and L_{BeF}, whereas L_{LiLi} increases sharply as indicated by Figure 3d. For LiF rich salt (95% LiF) the backscattering for Be−Be, Be−F, and F−F ion pairs diminishes significantly releasing the Be and F ions out of the trap and we observe considerable increase in the diffusion of these species. The Onsager coefficient of the ion pairs Li−Li, Li−F, and Li−Be increases significantly with the increase in LiF concentration. So as more and more LiF molecules are introduced in the mixture the movement of all of the species increases and the salt becomes more dynamic and free from any local entrapment.

We note that all the Onsager coefficients are $O(10^{-9})$ m^2/s, which is expected for typical ions in the liquid state. For binary system the Onsager coefficient follows the relation $L_{AA} = L_{BB} = -L_{AB}$, which leads to the fact that in pure LiF and in pure BeF_2 both the cation−cation and anion−anion pairs are in antiphase

DOI: 10.1021/acs.jpcb.5b04713
J. Phys. Chem. B 2015, 119, 10652−10663

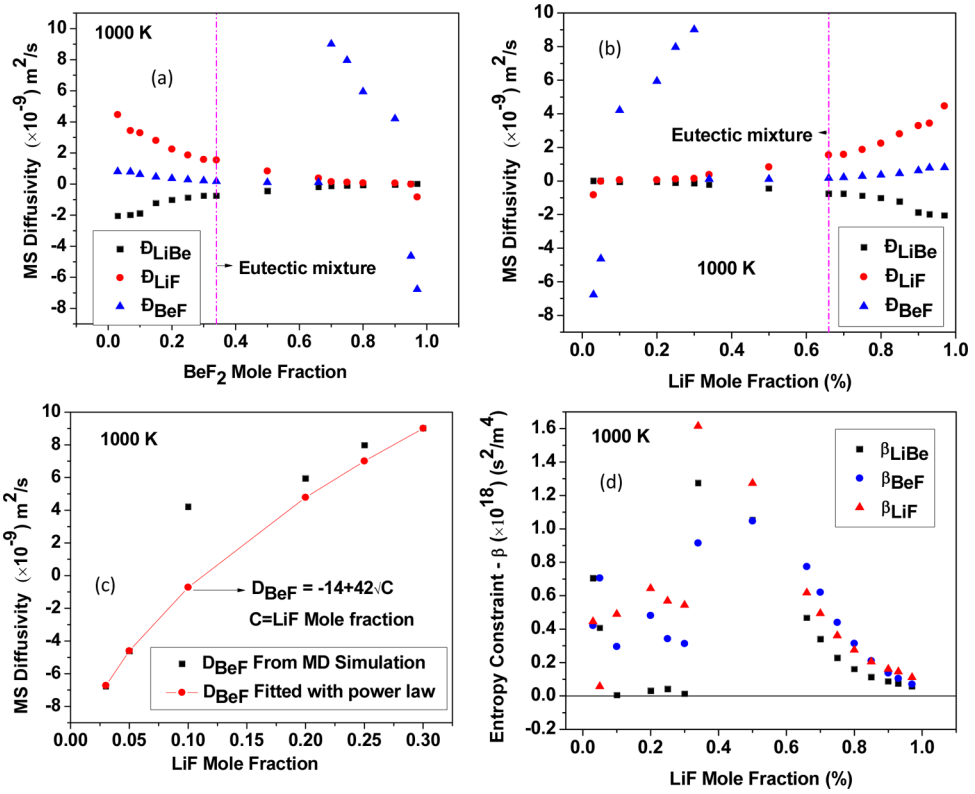

Figure 5. (a) Variation of MS diffusivities with mole fraction of BeF_2 at 1000 K, (b) Variation of MS diffusivities with mole fraction of LiF at 1000 K, (c) Sharp variation of $Đ_{BeF}$ on a magnified scale up to LiF mole fraction of 0.3, the red line plot is the fitted curve indicating that $Đ_{BeF}$ varies as square root of LiF mole fraction, (d) Variation of Entropy constraint with mole fraction of LiF at 1000 K showing a non-negative entropy production rate at all thernodynamic states.

(maxima of one correlation correspond to minima of other) with the corresponding cation−anion pair. In the BeF_2 rich mixture (5%LiF and 25% LiF), the correlation Be−Be is in antiphase with Be−F and F−F is in antiphase with Be−F. Once the mixture becomes LiF rich (LiF 66% and higher) the F−F correlation is not able to maintain its antiphase pattern with Be−F. Similarly Li−Li and F−F are able to maintain their dynamic antiphase pattern with Li−F for LiF rich composition and once the salt becomes BeF_2 rich (LiF 25% or below), F−F correlation fails to maintain its antiphase pattern with Li−F. So Flouride ions behave differently in the mixture relative to pure salt LiF or BeF_2. We can predict that the disappearance of antiphase between F−F and Be−F/Li−F may be attributed due to mixing.

4.2. Maxwell-Stefan Diffusivity. Figure 4a presents the variation of MS diffusivity with temperature for eutectic mixture (66% LiF). All three independent diffusivity, $Đ_{LiF}$, $Đ_{BeF}$, and $Đ_{LiBe}$ varies smoothly with the temperature and no divergence is observed. The diffusivity $Đ_{LiF}$, rises sharply with the temperature similar to the variation of Onsager coefficient L_{Li-F}. The rise in MS diffusivity with the temperature is consistent with the fact that viscosity of the eutectic mixture decreases with the temperature.[43] There is not much variation for the MS diffusivity between cation and anion pair $Đ_{BeF}$, which is supported by the fact that the Onsager coefficient L_{BeF} does not change much with the temperature. The interesting feature is that the MS diffusivity for cation pair $Đ_{LiBe}$ remains negative for the entire temperature range and its magnitude varies similar to $Đ_{LiF}$. Negative MS diffusivity for cation−cation pair although unusual have been reported experimentally for like−like ions in an exchange membrane system[29] and through MD simulations for molten salt LiCl−KCl where the diffusivity $Đ_{LiK}$ becomes negative and divergent.[10] Unlike LiCl−KCl system here we do not observe any diverging behavior for MS diffusivity. Negative MS diffusivity is not in violation of second law of thermodynamics, which demand that the total rate of entropy produced by all the diffusing species should be positive definite. The entropy production rate per unit volume is given by[14]

$$\dot{\sigma} = cR \sum_{\substack{i=1 \\ i>k}}^{n} \frac{x_i x_k}{Đ_{ik}} (\hat{\mathbf{U}}_i - \hat{\mathbf{U}}_k)^2 \tag{14}$$

where R is the universal gas constant. In order to have positive entropy production as given in eq 14 all the MS diffusivity cannot be negative at the same thermodynamic state. If one component of the multicomponent mixture undergoes an uphill diffusion by consuming entropy some other components of the mixture should produce entropy at such a rate that total entropy production remains positive.[14] Based on the constraints of the irreversible thermodynamics, the following inequality holds for all thermodynamic states[29]

$$\beta_{ab} = \sum_{\substack{i=1 \\ i\neq a}}^{n} \left(\frac{x_i x_a}{Đ_{ia}}\right) \sum_{\substack{j=1 \\ j\neq b}}^{n} \left(\frac{x_j x_b}{Đ_{jb}}\right) - \left(\frac{x_a x_b}{Đ_{ab}}\right)^2 \geq 0$$

$$a, b = (1, ..., n), a \neq b \tag{15}$$

For the ternary system LiF-BeF_2 there are three entropy constraints. We have carefuly computed all three entropy

DOI: 10.1021/acs.jpcb.5b04713
J. Phys. Chem. B 2015, 119, 10652−10663

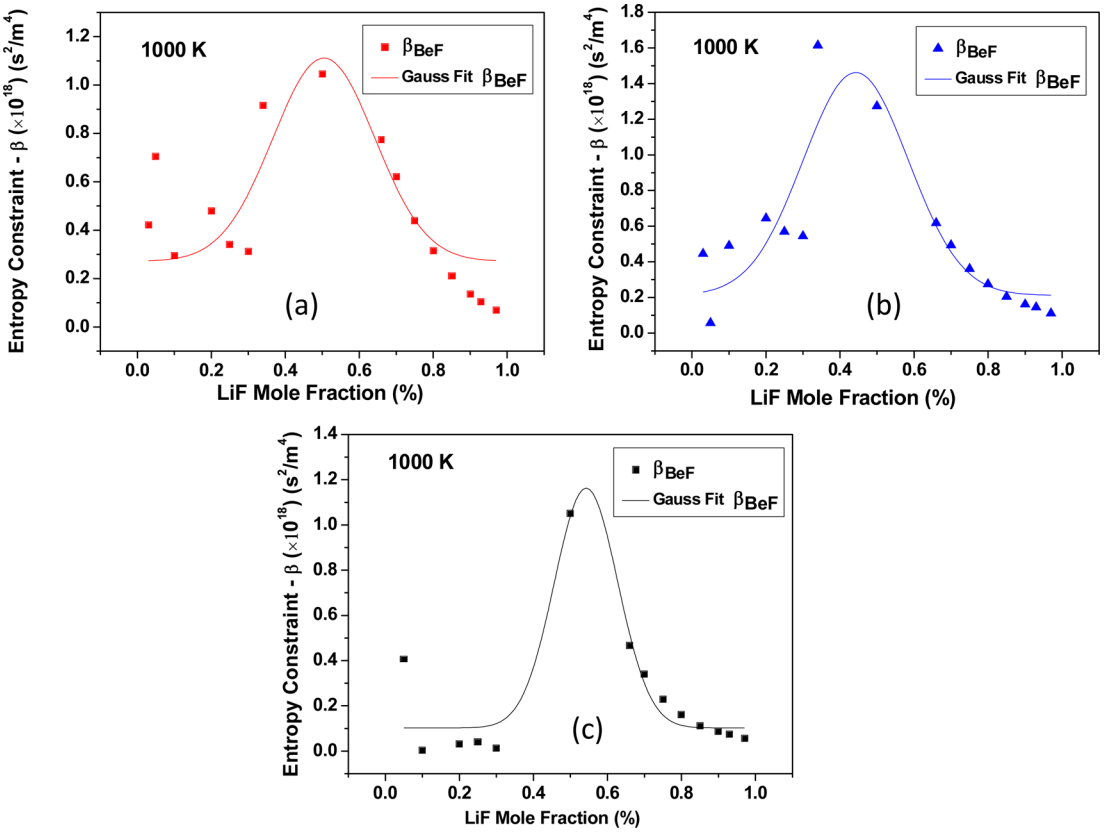

Figure 6. Gaussian fiiting of the entropy constraint with mole fraction of LiF at 1000 K.

constraints and plotted its variations with the temperature. We can see from the Figure 4b that entropy production rate remains non−negative at all temperature although MS diffusivity for positive-postive ion pair is negative.

Now we will discuss the variation of MS diffusivity with composition at a temperature of 1000 K as delineated in Figure 5. Although the MS diffusivities are expected to depend very lightly on the composition due to decoupling of thermodynamic factor here interesting composition dependence is seen. As we put BeF_2 in pure LiF, all the MS diffusivitiy decreases in magnitude with increase in mole fraction of BeF_2 as depicted in Figure 5a. There is a sharp rise of the MS diffusivity $Đ_{BeF}$, starting around 50% of BeF_2 which reaches maximum around 70% of BeF_2. Then it decreases almost sharply and strikingly even become negative at around 93% BeF_2. The sharp variation of $Đ_{BeF}$ may be attributed due to the fact that the short-range interaction of Be−F pair is stronger (only below to F−F pair) as shown in Figure 1 and the ion Be^{2+} has higher charge state compared to other ions leading to stronger long-range coulomb interactions. The MS diffusivity $Đ_{LiF}$ continue to decrease slowly as the composition becomes richer and richer in BeF_2 and finally becomes negative when LiF is less than 10% (5% and 3% LiF data). The MS diffusivity for cation−cation ion pair $Đ_{LiBe}$ is negative for LiF rich composition; its magnitude varies similar to $Đ_{LiF}$ and becomes positive around 93% of BeF_2. So we observe an interesting sign change for all three independent MS diffusivity around 93% the mole fraction of BeF_2.

In Figure 5b we have plotted the variation of MS diffusivitiy with LiF mole fraction for clarity. In order to focus on the sharp variation of $Đ_{BeF}$ with LiF mole fraction for low LiF%, in Figure 5c we present the variation of $Đ_{BeF}$ on a magnified scale up to LiF mole fraction of 0.3. We try to fit the simulated data with power law and find that for low LiF mole fraction $Đ_{BeF}$ can be best described as $Đ_{BeF} = -14 + 42\sqrt{C}$, where C is the mole fraction of LiF. So for low LiF mole fraction $Đ_{BeF}$ rises sharply with the square root of LiF mole fraction as shown by the red line in Figure 5c. This dependence can be related with the MS diffusivitiy between positive and negative ions ($Đ_{+-}$) in water solution where according to Debye−Huckel theory[44] $Đ_{+-}$ is proportional to square root of the salt concentration expressed as $Đ_{+-} \propto \sqrt{C_S}$, where C_S is the concentration of the salt. So $Đ_{BeF}$ follows the Debye−Huckel theory for low mole fraction of LiF.

4.3. Negative MS Diffusivity and Failure of Models. As the MS diffusivities are decoupled from thermodynamic factor it was believed that all the MS diffusivity should be positive, but after the observation of uphill diffusion by Duncan and Toor[45] the only constraint imposed is the positive entropy production governed by second law of thermodynamics. Although in electrolyte solution negative MS diffusivity was observed between positive ion pair here we report that MS diffusivity between cation−anion pair can also take any value and all the diffusivity can change sign at certain thermodynamic point. Overall the diffusion of all the species is higher when it contains maximum LiF. In order to asess the correctness of our computational data we have repeated the simulation by increasing the size of the supercell and taken so many independent runs with improved statistics. But in all the cases we observed similar trend. With the intention to see whether computed MS diffusivity satisfy the constraints of the irreversible thermodynamics imposed by second law of thermodynamics we computed entropy production rate for the diffusion of various species and plotted in Figure 5d. We can see that entropy production rate remains non-negative for

DOI: 10.1021/acs.jpcb.5b04713
J. Phys. Chem. B 2015, 119, 10652−10663

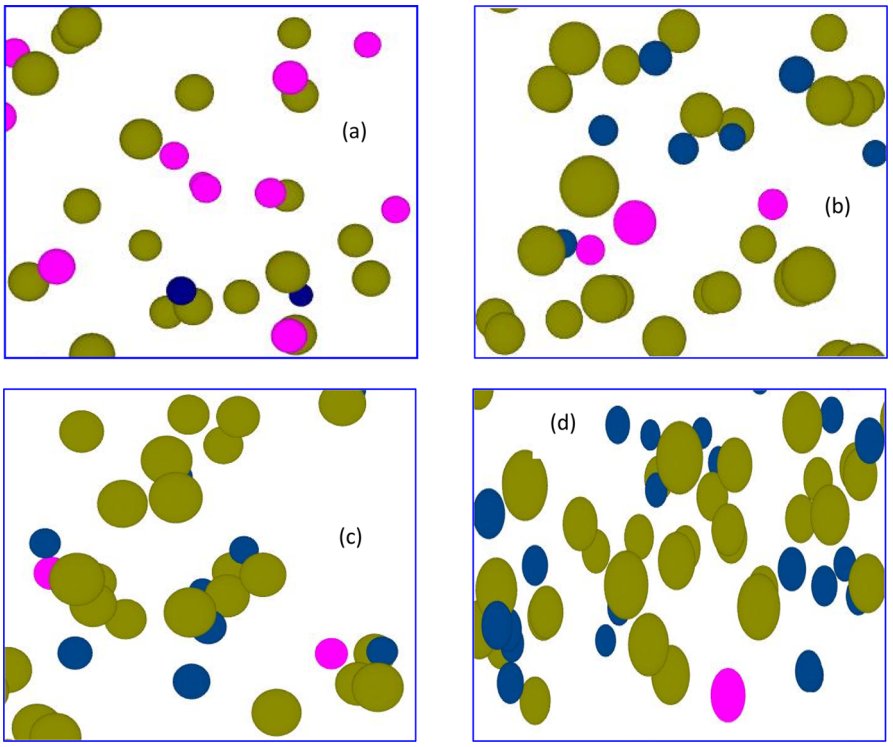

Figure 7. Structural snapshot of the salt mixture at 1000 K for various composition, (a) 80% LiF, (b) 25% LiF (c) and (d) 5% LiF; Pink, green, and blue color represents Li, Fe, and Be ions.

the entire composition even though all 3 MS diffusivity changes their sign when the mole fraction of BeF_2 is around 93%. Interestingly, the entropy production rate follows close to a Gaussian pattern for all three pairs. They are not true Gaussian, appears like asymmetric Gaussian. We try to fit those variations by Gaussian fitting and the fitted graphs are presented in Figure 6. We have thoroughly checked the literature and found from the work by Narebska[46] that for NaoH-Nafion system the MS diffusivity between cation−anion pair becomes negative for few cases for very low concentration of the salt. This supports our negative $Đ_{BeF}$ for very low concentration of LiF. The sign change for the MS diffusivity between cation−cation pair from negative to positive value is in agreement with the work of Kraaijeveld and Wesselingh[29] where they found that for like−like ion pair the diffusivities are usually negative at low concentration and may become positive at high concentration. The only exception is in the solution containing H^+ and solutions containing like ions of different valency where the MS diffusivity between cation−cation pair may deviate from general trend and become positive for the entire concentration range. Even though both negative and positive MS diffusivity do exist in the literature for both cation−cation and cation−anion pair in different systems we observe here all those interesting feature of both $Đ_{+-}$ and $Đ_{++}$ crossing the zero line and changing its sign in only LiF−BeF_2 system over the entire concentration range.

As comupting MS diffusivity for multicomponent system (ternary and higher) is very complicated and involves extensive computer simulaions so various models have been proposed to obtain MS diffusivity for multicomponent system from binary diffusion data. One of the popular model is based on generalized Vignes equation[23] where MS diffusivity between component i and j is given by

$$Đ_{ij} = (Đ_{ij}^{x_i \to 1})^{x_i} (Đ_{ij}^{x_j \to 1})^{x_j} \prod_{k=1, k\neq i,j}^{n} (Đ_{ij}^{x_k \to 1})^{x_k} \tag{16}$$

where $Đ_{ij}^{x_k \to 1}$ is the friction between the components i and j when both are diluted in component k. The quantity $Đ_{ij}^{x_k \to 1}$ cannot be obtained experimentally and several empirical models have been proposed to estimate $Đ_{ij}^{x_k \to 1}$ from binary diffusion data.[23] Another approach is to use generalized Darken equation, proposed by Krishna and Van Baten[34] where the concentration dependence of MS diffusivities in multicomponent mixtures based on molecular simulations of liquid mixtures is expressed as

$$Đ_{ij} = \frac{x_i}{x_i + x_j} D_{j,\text{self}} + \frac{x_j}{x_i + x_j} D_{i,\text{self}} \tag{17}$$

The self-diffusivities $D_{j,\text{self}}$ and $D_{i,\text{self}}$ are obtained from mass-weighted averages of the values at infinite dilution given by

$$D_{i,\text{self}} = \sum_{j=1}^{n} w_j D_{i,\text{self}}^{w \to 1} \tag{18}$$

The eq 17 is empirical and in systems with 3 or more components and in the limit where x_i and x_j are very very small it predicts that $Đ_{ij}^{x_k \to 1}$ will depends only on the ratio of x_i / x_j. This seems to be unphysical and can violates Onsager's reciprocal relations[47] as $Đ_{ij}^{x_k \to 1}$ is well-defined quantity and independent of the ratio x_i / x_j. A correct multicomponent Darken equation was derived by Liu et al.[48] and is expressed as

$$Đ_{ij} = \frac{D_{i,\text{self}} D_{j,\text{self}}}{D_{\text{mix}}} \text{ with } D_{\text{mix}} = \sum_{i=1}^{n} \frac{x_i}{D_{i,\text{self}}} \tag{19}$$

As the self-diffusion coefficients for binary mixtures are always postive the above models cannot provide negative MS

DOI: 10.1021/acs.jpcb.5b04713
J. Phys. Chem. B 2015, 119, 10652−10663

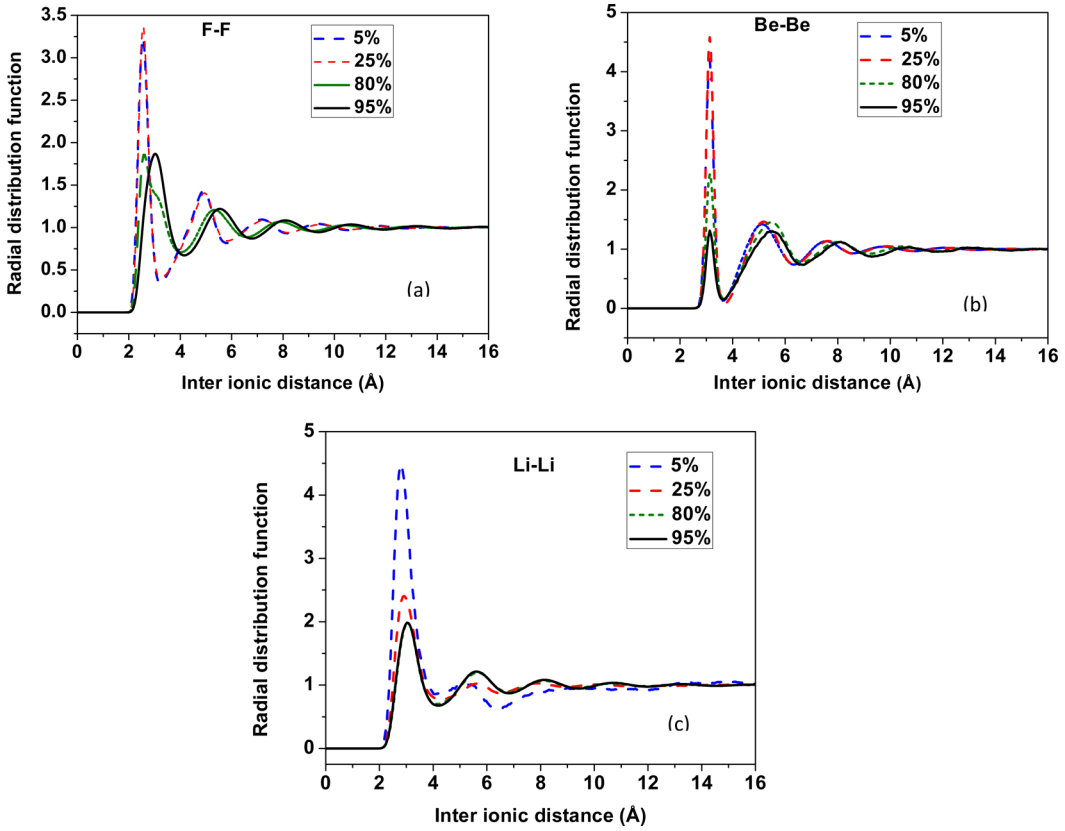

Figure 8. Radial distribution function for salt mixture with 5%, 25%, 80%, and 95% LiF at temperature 1000 K for the ion pairs (a) F−F, (b) Be−Be, and (c) Li−Li.

diffusivity as obtained for multicomponent electrolyte solutions. So the generalized Vignes equation and generalized Darken equation fails in LiF−BeF_2 and other electrolyte solution involving negative MS diffusivity. This is because in order to maintain charge neutrality the multicomponent electrolyte solution cannot be reduced to a set of binary systems but can only be reduced to a set of ternary system.[49]

4.4. Structure and Radial Distribution Function. Now we will try to correlate the structure and dynamics of the system for different thermodynamic states with the intention of explaining the unusual composition dependence of the MS diffusivity. As BeF_2 is introduced in pure LiF the diffusivity of the system goes down. This is due to the fact that the viscosity of BeF_2 is higher than that of LiF[50,51] and the presence of more and more BeF_2 molecules makes the system lethargic. But the striking feature is that around 66% of BeF_2, the MS diffusivity $Đ_{BeF}$ shows a sharp rise, reaches maximum value of around 9×10^{-9} m^2/s at 70% of BeF_2, and then decreases almost exponentially with a sign change for BeF_2 around 93%. What is the reason for such peculiar behavior of the MS diffusivity $Đ_{BeF}$ for BeF_2 rich salt? In order to put some light on this surprising variation of the MS diffusivity $Đ_{BeF}$, we look into the internal structure of the salt which leads to such interesting dynamics. Figure 7 presents the structural snapshot of the salt for 80%, 25%, and 5% LiF. We can see that at higher BeF_2 concentration the fluride ions reorganize to promote the formation of the tetrahedral fluoroberyllate network. At higher LiF%, there is no network formation and Li ions are surrounded by the fluride ions as well as Be ions are surrounded by fluride ions. As the BeF_2% increases there is strong tendency of F ions to come from the surrounding of Li ions and associate more and more around only Be ions to form network of fluoroberyllate with various charge states. The formation of fluoroberyllate network has been also observed by Serrano et al.[52] Due to this tendency of forming fluoroberyllate network F ions diffuse very fast from the surrounding of Li ions to be associated with the Be ions. This results in sharp rise in the MS diffusivity $Đ_{BeF}$. As the networks as a whole act as anion the Li ions now can move only around the network which restricted the diffusion of Li ions resulting in slow decrease in the diffusivity coefficient containing Li ions. As BeF_2% increases, the formation of higher degree of polymers, e.g, dimers $Be_2F_7^{3-}$, trimers $Be_3F_{10}^{4-}$, tetramers $Be_4F_{13}^{5-}$, etc., dominates over the monomer BeF_3^{-1}, which is predominately present in LiF rich mixture. We can note here that LiF acts as the bridging the flouride polyanion chains. So as Be and F ions are trapped inside the network of various flouride polyanion chains, the diffusivity of the species reduces sharply and they can only oscillate inside the network. This explains the sharp fall in the MS diffusivity $Đ_{BeF}$ when BeF_2 in the mixture exceeds 70%.

Once the network is formed Be and F ions are remain trapped inside the network and they oscillate back and forth. As the flouride ions move from various corners to be surrounded around Be to form higher degree of fluoroberyllate polymers the average F−F separation decreases. This is supported by the radial distribution function (RDF) as seen in Figure 8a. We can see that the position of first peak of RDF for F−F pair has reduced from 3.03 Å at 95% of LiF to 2.68 Å at 80% of LiF and finally to 2.57 Å at 25% of LiF mixture. Intenisty of first peaks also increases as the solution become rich in BeF_2 signifying that the association between the F−F pair becomes stronger

DOI: 10.1021/acs.jpcb.5b04713
J. Phys. Chem. B 2015, 119, 10652−10663

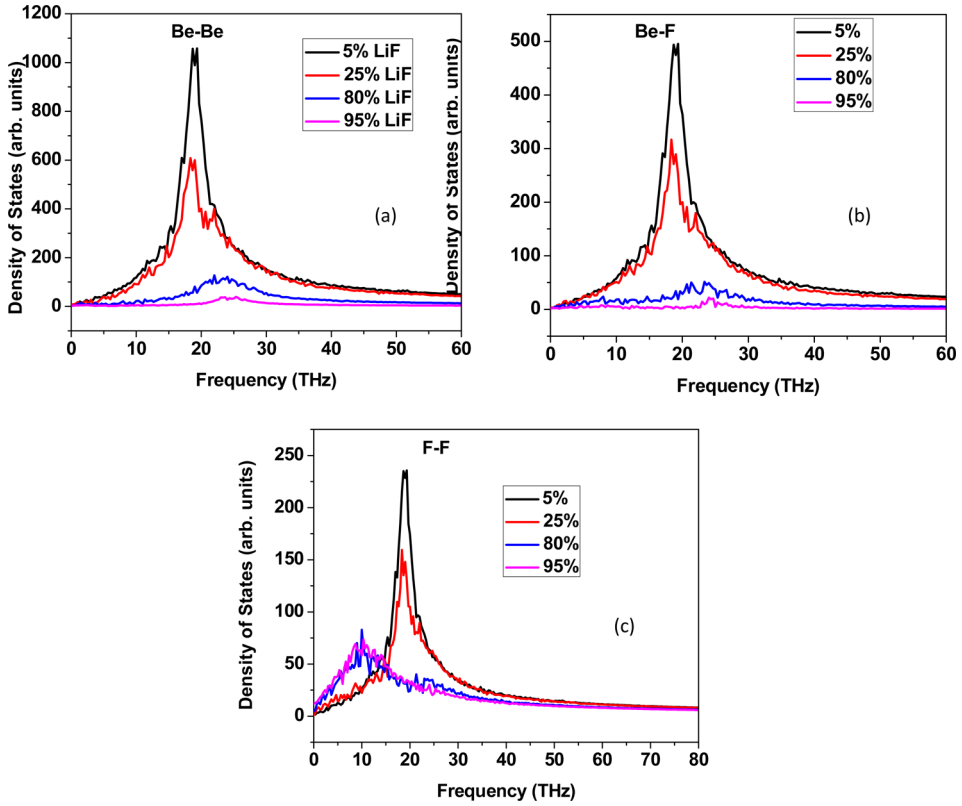

Figure 9. Vibrational density of states function for salt mixture with 5%, 25%, 80%, and 95% LiF at temperature 1000 K for the correlations between the ion pairs (a) F−F, (b) Be−Be, and (c) Li−Li.

and stronger due to formation of flouride polyanion network. There is sharpening of F−F peaks with increase in BeF_2% which also refelects formation of compact fluoroberyllate anions. Figure 8b shows that the intensity of first peak for Be−Be pair increases as mole fraction of BeF_2 increases. This may be attributed due to increase association of Be−Be pair as they organize to form flouride polyanion network when the mixture becomes rich in BeF_2. Spatial correlations between the Li ions increase as indicated by the increase intensity in Li−Li peak for higher BeF_2% as shown in Figure 8c.

4.5. Vibrational Density of States. To establish a correlation between the structure and dynamics in Figure 9, we present the vibrational density of states (VDOS) which is calculated from the Fourier transformation of the diffusive flux correlations. Interesting feature is that for Be−Be, Be−F and F−F correlations there is no change in peak frequency ($\nu^m \approx$ 19 THz) once the solution contains BeF_2 beyond 25%. This resembles a metastable phase independent of concentration signifying persistence of cage dynamics due to formation of fluoroberyllate network. Preservence of VDOS peak is supported by the prolonged and persistent backscattering in the diffusive flux correlations for Be−Be, Be−F and F−F pairs as seen in Figure 3. Interestingly for all three correlations the peak freuency is almost same ($\nu^m \approx$ 19 THz). We observe smearing of peak frequencies and broadening of the low frequencies with increasing LiF% which is consistent with the weakening of the cage dynamics. So we establish a strong relation between the structure and dynamics to explain the unusual composition dependence of MS diffusivity which has great impact on the performance of the reactor.

4.6. Signifacance of Negative MS Diffusivity. It is very difficult to get the physical significance and have a feel for negative diffusivity. From eq 2 we can say that the MS diffusivity $\mathcal{D}_{ij}$ acts as an inverse friction coefficient. So the negative diffusivity corresponds to negative friction coefficient. In general the materials have positive friction coefficient where the friction increases as we increase the normal force. If we press fingers gently on a table and slides across the surface it glides fairly easily. Once it is pressed hard it becomes difficult to slide as the firmer contact generates more friction. But for negative friction coefficient the friction decreases harder we push. The MS diffusivity, $\mathcal{D}_{BeF}$ becomes negative for BeF_2 rich salt with the formation of flouride polyanion network. With the formation of flouride polyanion network the association and the friction between Be and F increases. So we may expect that in this concentration region the normal force between Be and F would decrease in order to justify the negative friction coefficient. Negative friction coefficient has been reported with an atomic force microscope tip on graphite surface[53] where the friction decreases with increasing load.

4.7. Applications and Limitations. From coolant point of view, it is desriable that coolant should remove the heat more efficiently. In order to remove heat all the components should diffuse faster and there should not be any network formation. From Figure 5b, we can see that the magnitude of all three MS diffusivity starts increasing once LiF% is beyond 50% and becomes higher and higher beyond eutectic mixture. We have also computed the self-diffusion coefficients of various species for different composition as shown in Table 1. Computed self-diffusion coefficients of Li, F, and Be ions for eutectic mixture at 1000 K are 4.49, 1.59, and 1.10 in unit of 10^{-9} m^2 s^{-1}, respectively, which are in excellent agreement with the self-diffusion coefficients computed by Jabes et al.[9] using transferable rigid-ion model and polarizable ion potential. From the

DOI: 10.1021/acs.jpcb.5b04713
J. Phys. Chem. B 2015, 119, 10652−10663

Table 1. Self Diffusion Coefficients of Ions for Different Compostion at 1000 K

	self diffusion coefficients (10^{-9} m^2 s^{-1}) for various composition (LiF %)				
ions	5%	30%	67% (eutectic)	80%	95%
Li	6.94×10^{-02}	0.61	4.49	5.72	7.42
F	3.28×10^{-03}	0.33	1.59	2.89	5.59
Be	2.60×10^{-03}	0.01	1.10	1.95	3.09

Table 1, it is clear that the ions under the influence of electrical and activity gradient diffuse faster and faster as the salt becomes richer and richer in LiF. So from a diffusion point of view, we recommend to the experimentalist that little higher LiF% than eutectic (75−80% LiF) may be better choice provided little higher melting temperature can be accommodated. Increase of operating temperature has also the benefit of better thermal conductivity as the thermal conductivity increases with the temperature.[43]

In these simulations we have not considered the polarization effects which may be considered as a minor limitation. Taking into consideration that in our system Li^+ and F^- are monovalent species and only Be^{2+} is divalent species, the polarizability term may not be dominating as it is more important for multivalent species than for monovalent ones[54,55] Jabes et al.[9] studied the structure and transport properties of LiF-BeF_2 system using both transferable rigid-ion model and polarizable ion potential and predicted that the nonpolarizable, transferable rigid ion model presents reliable results for structural correlations and transport properties in comparison with first-principles-based, polarizable ion models (PIM). This justifies us to conclude that our prediction and qualitative trend of simulated data may be almost the same with the inclusion of polarization effects.

5. CONCLUSIONS

We observe a crossover in sign for all the MS diffusivity in ternary mixture LiF−BeF_2 at composition less than 10% LiF where the MS diffusivity between cation−anion pair ($Đ_{BeF}$ and $Đ_{LiF}$) jumps from a positive to negative value while the MS diffusivity between cation−cation pair ($Đ_{LiBe}$) becomes positive from a negative value. From the analysis of diffusive flux correlations, radial distribution function, structural snapshot, and vibrational density of states, we predict that the formation of flouride polyanion network between Be and F ions and coulomb interaction are responsible for the unusual composition dependence of MS diffusivity where the structure controls the dynamics. For a low mole fraction of LiF, $Đ_{BeF}$ follows the Debye−Huckel theory and rises with the square root of LiF mole fraction similar to the MS diffusivity between cation−anion pair in aquous solution of the electrolyte salt. As all three MS diffusivities can have both positive and negative value over the whole concentration range the various models which construct MS diffusivity for ternary and higher order system from binary diffusion coefficient fails for LiF−BeF_2 and other electrolyte solutions involving negative MS diffusivity. Since the magnitude of all three MS diffusivities starts increasing once LiF% is beyond 50% and becomes higher and higher beyond a eutectic mixture, from the difusion point of view to use LiF−BeF_2 as an efficient coolant, a little higher LiF% than eutectic (75−80% LiF) may be the better choice provided a corresponding higher melting temperature can be accommodated. Further investigations are needed to asses whether the composition point at which all three MS diffusivities change their sign is related to the critical mixing point of the mixture.

■ ASSOCIATED CONTENT

Supporting Information

The Supporting Information is available free of charge on the ACS Publications website at DOI: 10.1021/acs.jpcb.5b04713.

All the force field parameters used in the MD simulations (PDF)

■ AUTHOR INFORMATION

Corresponding Author

*E-mail: brahma@barc.gov.in. Phone: +91-2225592057.

Notes

The authors declare no competing financial interest.

■ ACKNOWLEDGMENTS

The author would like to thank Dr. S. M. Sharma for his constant support, encouragement, guidance, and useful discussions. The author would also like to thank Dr. Lavanya M. Ramaniah for her guidance and useful discussions. This work was possible due to the facilities, and help from the staff, of the BARC computer centre. The author would also like to thank Dr. Y. Sawant for useful discussions in curve fitting.

■ REFERENCES

(1) Grimes, W. R. Molten-Salt Reactor Chemistry. *Nucl. Appl. Technol.* **1970**, *8*, 137.

(2) http://fhr.nuc.berkeley.edu/wp-content/uploads/2014/09/AHTR.Nuclear.Technology.Article.May20.2003.pdf.

(3) http://allen.neep.wisc.edu/shell.

(4) Benes, O.; Konings, R. J. M. Thermodynamic properties and phase diagrams for fluoride salts for nuclear applications. *J. Fluorine Chem.* **2009**, *130*, 22−29.

(5) Matsumiya, M.; Takagi, R. A molecular dynamics simulation of the electric properties in molten chloride and fluoride quaternary systems. *Electrochim. Acta* **2001**, *46*, 3563−3572.

(6) Agarwal, M.; Sharma, R.; Chakravarty, C. Ionic melts with waterlike anomalies: Thermodynamic properties of liquid BeF2. *J. Chem. Phys.* **2007**, *127*, 164502−164511.

(7) Allen, M. P.; Tildesley, D. J. *Computer Simulation of Liquids*; Clarendon Press: Oxford, 1987.

(8) Sarou-Kanian, V.; Rollet, A. L.; Salanne, M.; Simon, C.; Bessada, C.; Madden, P. A. Diffusion coefficients and local structure in basic molten fluorides: in situ NMR measurements and molecular dynamics simulations. *Phys. Chem. Chem. Phys.* **2009**, *11*, 11501−11506.

(9) Jabes, B. S.; Agarwal, M.; Chakravarty, C. Structure and transport properties of LiF−BeF2 mixtures: Comparison of rigid and polarizable ion potentials. *J. Chem. Sci.* **2012**, *124*, 261−269.

(10) Chakraborty, B.; Wang, J.; Eapen, J. Multicomponent diffusion in molten LiCl-KCl: Dynamical correlations and divergent Maxwell-Stefan diffusivities. *Phys. Rev. E* **2013**, *87*, 052312−052318.

(11) Jolly, D. L.; Bearman, R. J. Molecular-dynamics simulation of the mutual and self diffusion coefficients in Lennard-Jones liquid mixtures. *Mol. Phys.* **1980**, *41*, 137−147.

(12) Schoen, M.; Hoheisel, C. The mutual diffusion coefficient D_{12} in binary liquid model mixtures. Molecular dynamics calculations ased on Lennard-Jones (12−6) potentials. *Mol. Phys.* **1984**, *52*, 1029−1042.

(13) Taylor, R.; Krishna, R. *Multicomponent mass transfer*, 1st ed.; Wiley: New York, 1993.

(14) Krishna, R.; Wesselingh, J. A. The Maxwell-Stefan approach to mass transfer. *Chem. Eng. Sci.* **1997**, *52*, 861−911.

(15) Bardow, A.; Kriesten, E.; Voda, M. A.; Casanova, F.; Blümich, B.; Marquardt, W. Prediction of multicomponent mutual diffusion in

DOI: 10.1021/acs.jpcb.5b04713
J. Phys. Chem. B 2015, 119, 10652−10663

liquids: model discrimination using NMR data. *Fluid Phase Equilib.* **2009**, *278*, 27−35.
(16) Cullinan, H. T., Jr. Analysis of Flux Equations of Multicomponent Diffusion. *Ind. Eng. Chem. Fundam.* **1965**, *4*, 133−139.
(17) Yao, Y. L. Algebraical Analysis of Diffusion Coefficients in Ternary Systems. *J. Chem. Phys.* **1966**, *45*, 110−115.
(18) Kirkaldy, J. S.; Weichert, D.; Haq, Z. U. Diffusion in multicomponent metallic systems. *Can. J. Phys.* **1963**, *41*, 2166−2173.
(19) Gupta, P. K.; Cooper, A., Jr. The [D] matrix for multicomponent diffusion. *Physica* **1971**, *54*, 39−59.
(20) Miller, D. G.; Vitagliano, V.; Sartorio, R. Some comments on multicomponent diffusion: Negative main term diffusion coefficients, Second Law constraints, solvent choices, and reference frame transformations. *J. Phys. Chem.* **1986**, *90*, 1509−1519.
(21) Vrentas, J. S.; Vrentas, C. M. Theoretical Aspects of Ternary Diffusion. *Ind. Eng. Chem. Res.* **2005**, *44*, 1112−1119.
(22) Helfferich, F. *Ion Exchange*; McGraw-Hill: New York, 1962; Chapter 6.
(23) Krishna, R.; Wesselingh, J. A. *Elements of Mass Transfer*; Ellis Horwood: Chichester, U.K., 1990; p 88.
(24) Lightfoot, E. N. *Transport Phenomenon and Living Systems*; Willey: New York, 1974; Chapter 3.
(25) Bothe, D. On the Maxwell-Stefan approach to multicomponent diffusion. *Prog. in Nonlin. Diff. Eqns. Appl.* **2011**, *80*, 81−93.
(26) Liu, X.; Schnell, S. K.; Simon, J.-M.; Bedeaux, D.; Kjelstrup, S.; Bardow, A.; Vlugt, T. J. H. Fick diffusion coefficients of liquid mixtures directly obtained from equilibrium molecular dynamics. *J. Phys. Chem. B* **2011**, *115*, 12921−12929.
(27) Liu, X.; et al. A. Fick Diffusion Coefficients in Ternary Liquid Systems from Equlibrium Molecular Dynamics Simulations. *Ind. Eng. Chem. Res.* **2012**, *51*, 10247−10258.
(28) Zhou, Y.; Miller, G. H. Green−Kubo formulas for mutual diffusion coefficients in multicomponent systems. *J. Phys. Chem.* **1996**, *100*, 5516−5524.
(29) Kraaijeveld, G.; Wesselingh, A. Negative Maxwell-Stefan diffusion coefficients. *Ind. Eng. Chem. Res.* **1993**, *32*, 738−742.
(30) Wheeler, D. R.; Newman, A. Molecular dynamics simulations of multicomponent diffusion. *J. Phys. Chem. B* **2004**, *108*, 18353−18361.
(31) Groot, S. R. D.; Mazur, P. *Nonequilibrium Thermodynamics*; Dover Publications, Inc.: New York, 1984.
(32) Hanley, H. J. M. *Transport Phenomena in Fluids*; Marcel Dekker: New York, 1969.
(33) Keffer, J.; Gao, C. Y.; Edwards, B. J. On the Relationship between Fickian Diffusivities at the Continuum and Molecular Levels. *J. Phys. Chem. B* **2005**, *109*, 5279−5288.
(34) Krishna, R.; van Baten, J. M. The Darken Relation for Multicomponent Diffusion in Liquid Mixtures of Linear Alkanes: An Investigation using Molecular Dynamics(MD) Simulations. *Ind. Eng. Chem. Res.* **2005**, *44*, 6939−6947.
(35) Todorov, I. T.; Smith, A. DL_POLY_3: the CCP5 national UK code for molecular-dynamics simulations. *W. Philos. Trans. R. Soc. London* **2004**, *A 362*, 1835.
(36) Martinez, L.; Andrade, R.; Birgin, E.G. J. M.; Martinez. Packmol: A package for building initial configurations for molecular dynamics simulations. *J. Comput. Chem.* **2009**, *30*, 2157−2164.
(37) Tosi, M. P.; Fumi, F. G. Ionic Sizes and the Born Repulsive Parameters in the NaCl-type alkali halides-II: The generalized Huggins-Mayer Form. *J. Phys. Chem. Solids* **1964**, *25*, 45−52.
(38) Ribeiro, M. C. C. Chemla effect in molten LiCl/KCl and LiF/KF mixtures. *J. Phys. Chem. B* **2003**, *107*, 4392−4402.
(39) Lantelme, F.; Turq, P. Ionic dynamics in the LiCl-KCl system at liquid state. *J. Chem. Phys.* **1982**, *77*, 3177−3187.
(40) Salanne, M.; Simon, C.; Turq, P.; Madden, P. A. Intermediate range chemical ordering of cations in simple molten alkali halides. *J. Phys.: Condens. Matter* **2008**, *20*, 332101.
(41) Rapaport, D. C. *The Art of Molecular Dynamics Simulations*; Cambridge University Press: Cambridge, 1995.
(42) Cantor, S.; Ward, W. T.; Moynthan, C. T. A. Viscosity and Density in Molten BeF_2-LiF Solutions. *J. Chem. Phys.* **1969**, *50*, 2874−2879.
(43) Williams, D. F. Assessment of Candidate Molten Salt Coolants for the NGNP/NHI Heat-Transfer Loop. 2006a, *Oak Ridge National Laboratory Report*, ORNL/TM-2006/69.
(44) Atkins, P. *Physical Chemistry*, 4th ed.; Oxford University Press: Oxford, 1990; p 275.
(45) Duncan, J. B.; Toor, H. L. An Experimental study of three component gas diffusion. *AIChE J.* **1962**, *8*, 38−41.
(46) Narebska, A.; Kajuawski, W.; Koter, S. Irreversible Thermodynamics of Transport across Charged Membranes. Part II. Ion-Water Interactions at Permeations of Alkalis. *J. Membr. Sci.* **1987**, *30*, 125−140.
(47) Liu, X.; Bardow, A.; Vlugt, T. J. H. Muticomponent Maxwell-Stefan Diffusivities at Infinite Dilution. *Ind. Eng. Chem. Res.* **2011**, *50*, 4776−4782.
(48) Liu, X.; Vlugt, T. J.H; Bardow, A. Predictive Darken Equation for Maxwell-Stefan Diffusivities in Multicomponent Mixtures. *Ind. Eng. Chem. Res.* **2011**, *50*, 10350−10358.
(49) Kraaijeveld, G.; Wesselingh, A.; Kuiken, G. D. C. Comments on "Negative Maxwell-Stefan Diffusion Coefficients. *Ind. Eng. Chem. Res.* **1994**, *33*, 750−751.
(50) Abe, Y.; Kosugiyama, O.; Nagashima, A. Viscosity of LiF-BeF, eutectic mixture (x_{BeF2}=0.328) and LiF single salt at elevated temperatures. *J. Nucl. Mater.* **1981**, *99*, 173−183.
(51) Merzlyakov, A. V.; Ignatiev, V. V.; Abalin, S. S. Viscosity of molten lithium, thorium and beryllium fluorides mixtures. *J. Nucl. Mater.* **2011**, *419*, 361−365.
(52) Serrano, A. R.; Lopez, M. H.; Zeifert, B.; Yanez, C. G. J. Thermodynamic analysis of LiF−BeF2 and KF−BeF2 melts by a structural model. *J. Fluorine Chem.* **2009**, *130*, 336−340.
(53) Deng, Z.; Smolyanitsky, A.; Li, Q.; Feng, X. Q.; Cannara, R.J. A. Adhesion-dependent negative friction coefficient on chemically modified graphite at the nanoscale. *Nat. Mater.* **2012**, *11*, 1032−1037.
(54) Salanne, M.; Madden, P. A. Polarization effects in ionic solids and melts. *Mol. Phys.* **2011**, *109*, 2299−2315.
(55) Ohtori, N.; Salanne, M.; Madden, P. A. Calculations of the thermal conductivities of ionic materials by simulation with polarizable interaction potentials. *J. Chem. Phys.* **2009**, *130*, 104507−104513.

DOI: 10.1021/acs.jpcb.5b04713
J. Phys. Chem. B 2015, 119, 10652−10663